Biocatalytic stereocontrolled head-to-tail cyclizations as a tool for streamlined hybrid synthesis of terpenes

Andreas Schneider[1], Thomas B. Lystbæk[1], Daniel Markthaler[2], Niels Hansen[2] & Bernhard Hauer[1]*

[1]Institute of Biochemistry and Technical Biochemistry, University of Stuttgart, Stuttgart-Vaihingen, Germany

[2]Institute of Thermodynamics and Thermal Process Engineering, University of Stuttgart, Stuttgart-Vaihingen, Germany

Abstract

The stereocontrolled cationic cyclization cascade is a vital step in the modular biogenesis of terpenes, as it defines the carbon skeleton's three-dimensional structure in one atom-economical step. While nature has adopted this strategy for eons, state-of-the-art synthetic routes to asymmetrically access cyclic terpenes still rely predominantly on sequential multi-step scaffold remodelling. Herein, we bridge this long-standing methodological gap by unlocking the target-oriented synthesis ability of the squalene-hopene cyclase. Our mechanistic insights show that the biocatalytic head-to-tail cyclization is highly customizable by mechanism-guided enzyme engineering and substrate-focused setup engineering. As a result, we demonstrate two- or three-step hybrid synthetic routes of pheromones, fragrances, and drug candidates by merging a stereocontrolled cyclization with interdisciplinary synthetic and catalytic methods. This biomimetic strategy significantly reduces the synthesis effort to terpenes and provides rapid access to thousands of head-to-tail-fused scaffolds.

Keywords: terpenes, cation-olefin cyclization, biocatalysis, squalene-hopene cyclase, new-to-nature conditions, hybrid synthesis

Introduction

Chemoenzymatic hybrid synthesis is an aspiring paradigm, which synergistically merges the advantages of biocatalysis and state-of-the-art synthesis to streamline the access to complex (natural) molecules.[1,2] Terpenes belong to nature's most sophisticated and diverse library of molecular scaffolds and find increasing application as biosubstitutes in vital areas e.g., energy as battery parts or biofuels, as well as human health and well-being.[3,4] For the latter in particular, a precisely arranged three-dimensional carbon skeleton is of utmost importance as it facilitates specific substrate recognition in biological receptors such as the human nose or pathogens. Thus, accessing terpenes in a stereocontrolled manner developed into its own field of organic chemistry and created a fountain of chemical creativity in retrosynthetic logic.[5] In their endeavor to generate complex terpenes, the Renata group demonstrated the power of chemoenzymatic terpene synthesis by successfully implementing the regio- and stereoselective remote oxyfunctionalization ability of oxygenases into their synthesis routes.[6] This development opened up entirely new retrosynthetic considerations in terpene synthesis through a reinvigoration of the chiral pool.[7] However, it is this 'chiral pool'[8] or 'scaffold remodelling' (SR)[9] strategy that renders access to cyclic terpenes complicated. In particular, this approach often entails low atom economy and overall low efficiency caused by strategic functional group manipulation and sequential chemistry (Fig. 1a, Route A). It is therefore not surprising, that despite their huge potential as bioactive compounds, terpenes are still highly underrepresented e.g., in Pharma (1.3% of APIs)[10], as they are mainly produced via metabolic engineering of organisms or are extracted from overexploited plants with low biomass efficiency (usually 1-5% of plant material).[11,12]

To overcome this dichotomy, a *de novo* synthesis including a target-oriented and stereocontrolled cationic cyclization of the natural achiral linear precursor would dramatically shorten synthetic routes to cyclic terpenes (Fig. 1a, cf. Fig. S1). Nature uses this strategy for eons[13] and despite the tremendous progress in the field of biomimetic stereocontrolled head-to-tail cyclization employing diverse catalysts e.g., Brønsted-acids[14], transition metals[15] or

supramolecular cages[16], their application in terpene synthesis is still highly underrepresented (<1%, Table S1). This is due to frequently required cryogenic conditions, alternative initiation motifs, limited stereocontrol, and inevitable strong nucleophiles as terminating groups of the cyclization, which collectively also excludes the use of broadly abundant natural linear precursors (Fig. 1a, Route B).[17] In contrast, cyclases can activate prenyl-moieties and guide the highly reactive cationic intermediates through a chiral cation cage to their final destination with unparalleled selectivity at ambient conditions.[18] To streamline the access to cyclic terpenes, we thus envisioned unlocking their unique catalytic capabilities for the target-oriented chemoenzymatic hybrid synthesis of terpenes.

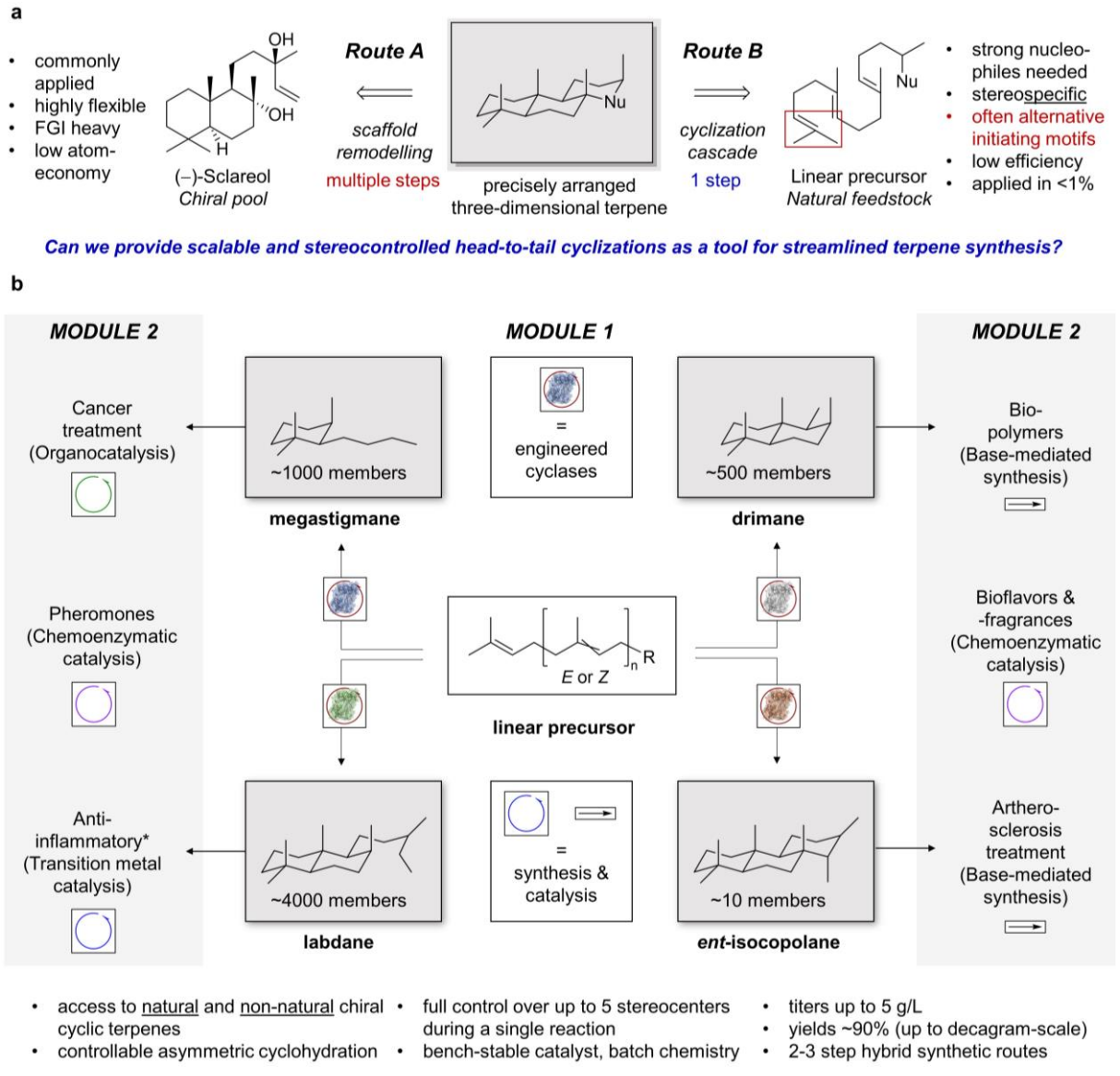

Figure 1: State-of-the-art strategies in terpene synthesis. (A) Traditional chemical strategies include commonly applied multi-step 'chiral pool' or 'scaffold remodelling' approaches and scarcely applied single step cationic

cyclization cascade. (B) The presented modular hybrid strategy includes target-oreinted cyclase biocatalysis for scaffold diversification and interdisciplinary synthesis and catalysis for scaffold derivatization. *not generated in this study.

Herein, we report on the realization of this endeavor by embracing the exquisite biocatalysis of the squalene-hopene cyclase (SHC). At the outset of this work, the promiscuity and application strategies of SHCs for specific targets have been demonstrated, which usually required tedious isolation protocols or huge host cell amounts (~400 g/L).[19,20] However, a comprehensive study on systematically enabling and showcasing their synthetic utility on a broad substrate scope, entailing the drastic change in step-efficiency in terpene synthesis has yet to be addressed. Our aim was to mimic nature's elegant and modular divergent synthesis strategy,[21] employing SHCs in the scaffold diversification (Fig. 1b, Module 1), which installs all desired stereocenters in one step. The generated megastigmane, drimane, labdane, and *ent*-isocopolane scaffolds share their skeleton with >5000 natural products which constitutes the divergence potential of this hybrid strategy.[22] Using interdisciplinary synthesis and catalysis for scaffold derivatization, finally, should enable highly efficient synthetic routes to diverse terpenes (Fig. 1b, Module 2).

Generation of cyclic terpene precursors by engineered SHCs

To put our outlined plan into action, we selected targets from diverse areas of application, varying in their carbon skeleton size and complexity (Fig. 2a, black structures). Actinidiolide **1** derivatives are prominent bioflavors and insect pheromones, and require a non-trivial formal insertion of an oxygen into the monocyclic skeleton of cyclohomogeranial.[23] 1,3-dioxanone **2** can be derived by carbonylation of a drimane diol and transformed into biodegradable polymers with a tailored chiral backbone as used e.g., in tissue engineering.[24] Metachromin **3** is applied in hepatitis[25] or cancer treatment[26] studies and combines the megastigmane skeleton with 2-acetyl-resorcinol. The privileged meroterpene hybrid structure combines a three-dimensional terpene skeleton with a flat aromatic moiety, which renders it promising as a bioactive compound.[27] Another representative of this compound family is the sponge-derived meroterpene **4** that bears potential in inflammation disease treatment[28] and

can be fused by the tricyclic *ent*-isocopalane skeleton and p-hydroxy-benzoic acid. The last and most complex targets, the α-pyrone meroterpenes **5** offer a promising broad range of biological activities[29] and can be dissected into a sclareoloxide-like β-keto ester structure and an arene moiety. We are aware that the targets presented herein lack functionalizations, such as the OH-group at position C-3 of **5**. One the one hand, this circumstance emphasizes the important contributions of the Baran[30] and the Renata group in the field of terpene oxidations.[6] On the other hand, the focus of this work was to showcase the synthetic potential of the SHC *en* route to terpenes, which is why prior, or late-stage oxidations were not considered.

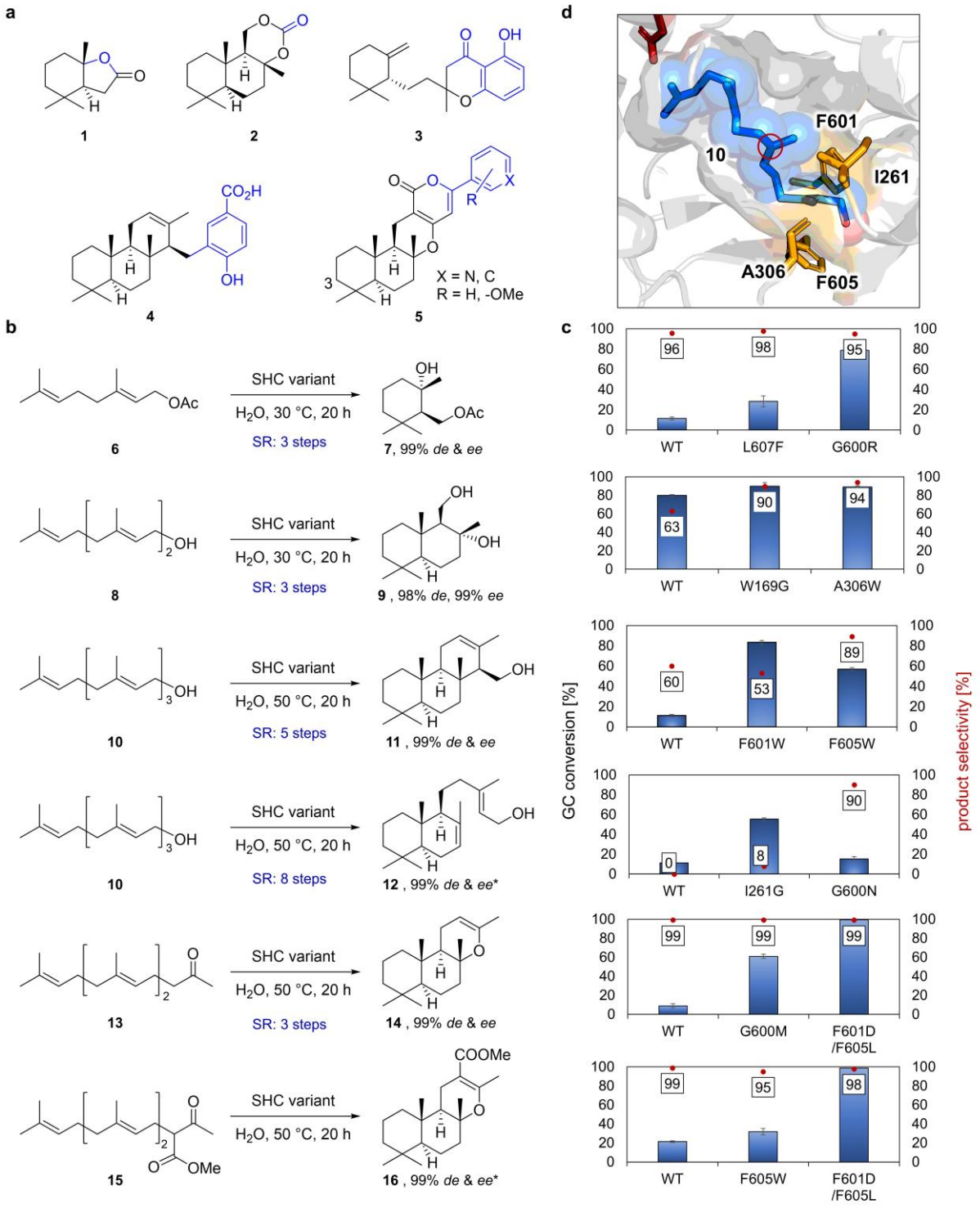

Figure 2: Terpene targets and accessing their terpene skeleton by engineered SHCs. (A) Selected cyclic terpenes 1-5 from different areas of application,[23–29] their terpene skeleton (black) and the additionally required functionality (blue). (B) Linear terpene precursors selctively cyclized by engineered SHC variants to the desired cyclic scaffolds in analytical biotransformations. SR = scaffold remodelling. * assumed due to shape-complementary substrate prefolding in the SHC active site (Fig. S2) and circular dichroism data. Please see supporting information for reaction details. (C) GC conversion and product selectivities of the best hits compared to the AacSHC wildtype (WT) as determined from the area of the GC-FID peaks (cf. Fig. S3-S9). (D) Substrate 10, shown as blue sticks and spheres, docked in the confined active site of the *Aac*SHC (PDB: 1UMP) exemplifies the generally observed pre-folding of all substrates. Most identified beneficial mutations are positioned in a sphere around the terpene's functional group (orange sticks). This can be leveraged as a mutagenesis strategy of these enzymes.

With these retrosynthetic analyses in mind, we commenced screening our in-house SHC library with the appropriate linear terpenes starting from the smallest one *E*-geranyl acetate **6** (Fig. 2b). Biotransformations were carried out *in vivo* as this setup proved its efficiency for the membrane-bound enzyme (Fig. 2c).[31] All substrates were also evaluated *in silico* by docking them into the confined active site of the *Aac*SHC wildtype (Fig. 2d and Fig. S2) and learning from substrate-mutant combinations. A stereoselective cyclohydration of **6** would directly provide the precursor cyclogeranyl acetate hydrate **7** for the synthesis of **1** and thus overcome the three-step SR.[23] To our delight the wild-type (WT) *Aac*SHC and mutants at positions G600 and L607 already exhibited this promiscuous ability, however, also produced moderate amounts of solvolysis product geraniol (Fig. 34). Variant G600R shifted this product ratio to >90% in favor of the cyclohydration product and boosted the enzymatic activity 7-fold.

Moving along the isoprene chain length, another stereoselective cyclohydration of sesquiterpene *E*,*E*-farnesol **8** would result in the desired drimane skeleton for dioxanone **3** formation and shorten concurrent SR routes by two steps.[32] While this substrate has already been the target of *Aac*SHC-mediated cyclization by Hoshino and Hauer[33,34], those studies employed purified enzyme and identified variants that lacked full selectivity and conversion of **8**, respectively. We discovered multiple novel hit positions mostly around the substrate's alcohol moiety (cf. Fig. S4), of which variant A306W achieved high conversion (89%) and excellent drimen diol **9** selectivities (94%). Notably, we found variant L36V/Y420F/G600L that enabled the stereocontrol of the final hydration and provided the opposite diastereoisomer **S1-9** of drimen diol **9** with a diastereoselectivity of 88% (Fig. S4 and NMR data).

In view of the sponge-derived meroterpene **4**, we next focused on the cyclization of linear diterpene *E*,*E*,*E*-geranyl geraniol **10**. Hoshino and co-workers reported the promiscuous tricyclization of **10** to **11** using purified *Aac*SHC WT, albeit with a low yield of 12%[34], and biocatalytic access to labdane diterpenes was reported by the Peters group but required the extraction of 3L fermentation broth and yielded only 3 mg product.[35] Our aim, therefore, was to direct the cyclization of **10** towards both products with high selectivity and high conversion

using engineered SHCs. Regarding the tricyclization, beneficial mutations were identified at positions F601 and F605. It turned out that most of the hits, e.g., F601W were more active (up to 8-fold) than the WT but lacked selectivity towards **11** (Fig. S5). However, variant F605W produced the α-product *ent*-isocopolol **11** with 5-fold improved conversion and ~90% selectivity. Favoring bicyclization of **10** was achieved by mutations at I261, G600, and L607 that are located around the third transient carbocation (Fig. 2d, red circle). Congruent to the tricyclization, most variants yielded product mixtures that emphasizes the challenge of selective cyclizations even with an enzyme (Fig. S5). Merely, the asparagine at position 600 resulted in high (90%) selectivity towards the bicyclic labdane scaffold **12** with a conversion comparable to the WT. Interestingly, the *in silico* docked product **12** in computationally generated variant G600N gives rise to a dual function of the asparagine that is anchoring the functional group[31] and acting as a Brønsted-base (Fig. S6).[36] Labrotary efforts towards ent-isocopolol **11** and labdanol **12** encompass 5 and 8 steps, respectively.[37,38]

Coming to our last target, the α-pyrone meroterpenes **5**, we drew inspiration from a study by Parker et al.[39] which used a non-natural sclareoloxide-like terpene structure that was racemically cyclized using electrophilic mercury. In preparation for this transformation, we evaluated the cyclization of *E*,*E*-farnesyl acetone **13** to sclareoloxide **14** with our SHC library. We chose this strategy due to the fact that the natural substrate **13** and the non-natural linear precursor **15** are almost identically pre-folded in the active site of the *Aac*SHC WT (cf. Fig. S3e and f). Hit variants for **13** should then be tested with **15** to save time and resources. Promiscuous cyclization of **13** towards sclareoloxide **14** with purified *Aac*SHC has been reported, albeit with very low conversions below 1%.[40] Our survey yielded variant F601D/F605L, among multiple other hits (Fig. S7), which surpassed the WT 10-fold, while ensuring high selectivity. Curiously, the amino acid exchanges F601D and F605L both presumably result in less confinement around the keto-group of **13** in the active site, which is contrary to the increased conversion at first glance. However, the introduced aspartate may anchor the keto-group and therefore lock the substrate in the right pre-folding faster or act as Brønsted-base to activate the final nucleophile. Subsequently, we used the non-natural linear

precursor **15** with the distinguished SHC variants. Notably, we noticed that **15** is prone to decarboxylate to **13** (Fig. S8), thus the Brønsted-acid catalyst has to overcome this side reaction and, moreover, select one out of three potential final nucleophiles. Intriguingly, variant F601D/F605L exhibited excellent conversion (99%, 5-fold higher compared to WT) and selectivity (98%) towards the desired cyclic product **16**, which emphasizes the reliability of our docking results and highlights the precise catalyst control of the SHC. Cyclic **14** can be prepared by SR in 3 steps[41] whereas **16** has only been racemically cyclized yet.

In summary, we were able to produce all desired (and more in the SI) carbon scaffolds with high conversions and excellent selectivities, empowered by the tunable shape-complementary pre-folding of substrates in the confined active site of the biocatalyst. Our data demonstrate that mechanism-guided enzyme engineering in the sphere around the desired transient carbocation, as showcased for substrate **10** in Fig. 2d, enables the direction of cationic head-to-tail cyclizations in terms of regioselective deprotonation, stereoselective hydration, and cascade progress. Leveraging this knowledge paves the way to the cyclization of dozens of carbon skeletons with divergence potential to tens of thousands of natural products using the SHC.[22] To the best of our knowledge there is no chemical catalyst that is able to control the cyclization of these unbiased terpenes to such an extent (cf. Table S2 and supporting chromatograms), especially with an alkene as the terminal nucleophile (substrates **6**, **8**, **10**). A limitation of the presented strategy is that, surprisingly, no single β-deprotonation product could be detected.

Technical and mechanistic investigations on the biocatalyst preparation

Having ascertained the stereocontrolled formation of the carbon skeleton, we intended to provide a concise setup to translate SHC biocatalysis from lab to liter scale. As nature usually operates far beyond industrially relevant substrate titers, scalable biocatalysis requires precise evaluation of the requisite new-to-nature conditions and the enzyme per se.[42] The topology of monotopic membrane-enzymes, as the SHC, constitute only 0.06% of nonredundant protein structures and are permanently dependent on their biological host's

membrane.[43] Taking this into account, the application of these enzymes as a whole-cell biocatalyst becomes apparent as it circumvents tedious isolation and use of membrane mimics. As a model reaction for initial investigations, we chose the broadly studied promiscuous cyclization of *E*-geranyl acetone **17** using *Aac*SHC variant G600M[31] (Fig. 3a). First, we proved the ability to use lyophilized *E. coli* whole-cells, which would drastically simplify the storability and application of these enzymes as a powder. To our delight, biotransformations showed no difference in conversion and long-term stability (Fig. 3b). To improve substrate availability, four cyclodextrins were tested, which disclosed 2-hydroxypropyl-β-cyclodextrin (2HPβCD) as the best candidate that improved the conversion 2-fold (Fig. S9). Next, we proved scalability employing a protocol that we elaborated previously[31] using 5 g/L (25 mM) substrate, 10 g_{CDW}/L cells, 14 g/L (10 mM) 2HPβCD and buffer in a 5 L reactor stirring with 100 rpm at 30 °C what demonstrated a slow but operationally stable catalyst for 84 days and yielded 22.4 g (90%) of cyclic **18** (Fig. 3c).

Having solved the technical issues, we questioned the constitution of our biocatalyst, and its long-term storage as well as operational stability. Comparing the growth of freshly expressed cells with the lyophilized ones on an Agar-plate disclosed that few cells survive the lyophilization process. This fact was further illuminated via fluorescence microscopy which showed that mainly cell debris remains (cf. Fig 3d and e, also see Fig. S10). These experiments thus explained that the SHC does not require a viable cell but parts of the cell membrane, where the enzyme is embedded (see Thermolysis protocol in the supporting information), are enough to drive the biocatalysis.

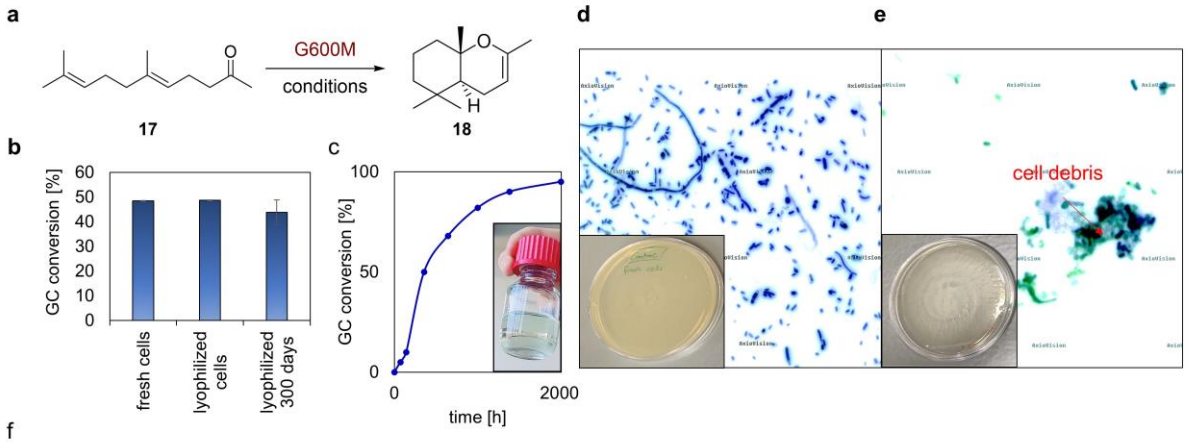

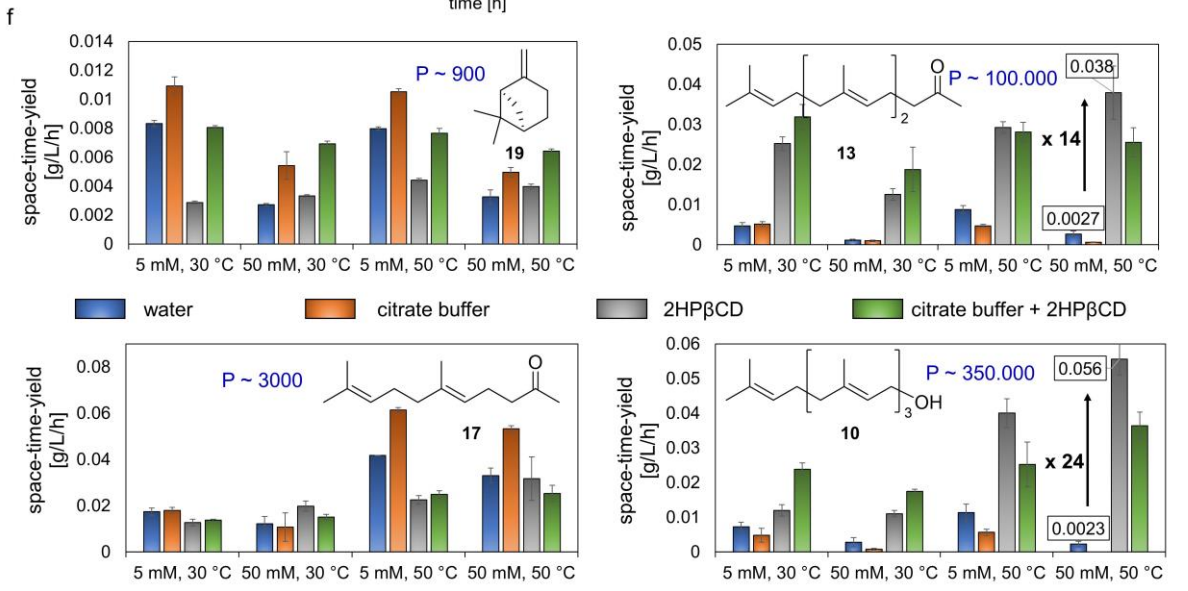

h

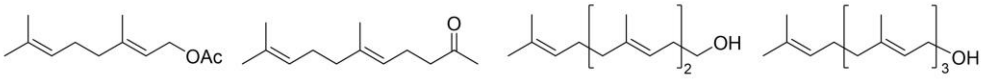

	6	17	21	10
$\Delta G_{solv}H_2O$ [kJ/mol]	-15.3	-13.2	-9.5	-7.9
$\Delta G_{H2O \rightarrow 2HP\beta CD}$ [kJ/mol]	-35.9	-40.2	-47.3	-51.1
$\Delta G_{H2O \rightarrow CH}$ [kJ/mol]	-32.8	-34.1	-45.6	-60.3

Figure 3: Establishing a concise and comprehensible setup for scaling up *'in vivo'* SHC biocatalysis. (A) Model reaction for intial experiments. (B) Comparison of freshly expressed cells, lyophilized cells and stored lyophilized cells by employing the model reaction. (C) Time-conversion curve of the model reaction in a 5L reactor and the isolated product. (D) Freshly expressed *E. coli* cells after 16 h of incubation on an Agar-plate and under the fluorescence microscope show highly abundant and viable cells (please see Fig. S11 for more details). (E) Lyophilized *E. coli* cells after 16 h incubation on an Agar-plate and under the fluorescence microscope show no growth on the plate and predominatly cell membrane debris. (F) Space-time-yield of analytical biotransformations using (+)-β-pinene 19 (TelSHC C312S), *E*-geranyl acetone 17 (AacSHC G600M), *E*,*E*-farnesyl acetone 13 (AacSHC F601D/F605L) and *E*,*E*,*E*-geranyl geraniol 10 (AacSHC F605W) under varying substrate concentrations and temperatures in water, 100 mM citrate buffer (pH = 6.0), 50 mM 2-hydroxypropyl-β-cyclodextrin (2HPβCD) and 100 mM citrate buffer (pH = 6.0) + 50 mM 2HPβCD. Partition P = [octanol/water] calculated by ChemDraw is given as blue numbers. High number means high hydrophobicity. (H) Free energy calculations of the transfer free energy of substrates 6, 17, 21 and 10 from water into 2HPβCD and cyclohexane set as artificial membrane (for justification see computational methods in the supporting information). For reaction details of analytical biotransformations, calculation parameters and controls please see supporting information.

Intrigued by this data, we next examined parameters that may influence the space-time-yield of the biocatalysis using terpenes. Buffer, cyclodextrin and the combination thereof were evaluated as additives. Moreover, terpene type (as defined by their partition coefficient P = [octanol/water], Fig. 3f, blue numbers), terpene concentration, cell concentration, and temperature were evaluated to get a coherent picture (Fig. 3f). To keep catalyst loading low we used 10 g_{CDW}/L cells in all setups. The more hydrophilic terpenes (+)-β-pinene **19** and *E*-geranyl acetone **17** were better converted to (+)-α-pinene **20** and *trans*-hexahydrochromene **18**, respectively, in the presence of the chelating citrate buffer (cf. Fig. S11 for non-chelating buffer). Vice versa the more (~100-400-fold) hydrophobic substrates **13** and **10** were generally better cyclized to **14** and **11**, respectively, in the presence of encapsulating 2HPβCD. Combining buffer and 2HPβCD was beneficial for the more hydrophobic substrates (**13** and **10**) at 30 °C and substrate **19** at high substrate concentrations and temperatures. Noteworthy, high hydrophobic substrate concentration in the absence of 2HPβCD was mostly deleterious on the enzymatic activity, especially for substrate **10** at elevated temperature, which completely disrupted the activity in the buffer. Increasing the cell concentration 5-fold, positively affected the conversion of substrate **17** and highly hydrophobic substrate **10** at 30 °C (Fig. S12). Intuitively, the beneficial effect of 2HPβCD rises with increasing P of the substrates (Fig. S13) and, finally, it is generally advisable to employ a thermostable enzyme variant at higher substrate concentrations, which is known correlation[44] (Fig. S14). Tempted by the substrate-dependent effects of 2HPβCD in our setup, we calculated the transfer free energies of the increasingly hydrophobic substrates geranyl acetate **6**, geranyl acetone **17**, homofarnesol **21**, geranyl geraniol **10** from water into the core of 2HPβCD versus the into the membrane, where the enzyme naturally sources its substrates, using the double decoupling method (for more information and selected calculated products, such as ambroxide **22,** see supporting information). This data disclosed that (a) membrane partition and encapsulation of terpenes by 2HPβCD is generally beneficial for the system (cf. $\Delta G_{solv}H_2O$ vs. $\Delta G_{H2O\rightarrow 2HP\beta CD}$ and $\Delta G_{H2O\rightarrow CH}$) (b) both partitions are competing processes and (c) for more hydrophilic substrates the encapsulation by 2HPβCD is stronger than partition into the membrane and (d) that with

increasing hydrophobicity partition into the membrane becomes more beneficial than being encapsulated. It should be noted that both transfers are reversible processes.

To sum up, our comprehensive data set disclosed that the SHC is independent of a viable cell, which ensures long-term storage as well as operational stability. However, the setup is largely dependent on the sum of abiotic stressors, such as temperature, buffer, and terpenes, acting on the system, which consists of the membrane and the membrane-bound enzyme (Fig. S15). The pivot herein is to recognize the substrate's level of hydrophobicity and based on that augment biocatalysis by setting the other parameters with special focus on temperature and internal organic reservoirs such as cyclodextrin. The host molecule not only improves the solubility of the hydrophobic molecules but also weakens their deleterious effect on the bioconversion by reversible encapsulation. Vice versa the encapsulation is mostly deleterious for more hydrophilic substrates at the chosen conditions. It should be noted that two-phase systems with several solvents were also tried what did not result in improved biocatalysis (data not shown). These findings emphasize the practicability and flexibility of the biocatalyst setup for synthetic purposes.

Implementing stereocontrolled head-to-tail cyclizations into hybrid synthetic routes

The elaborate substrate-focused protocol thus paved the way for the final objective of this work: The hybrid syntheses of the terpenes devised in Fig 2a by mimicking nature's modular strategy (Fig. 4). Lactone terpenes, such as **1**, are usually prepared via C-1 homologation of the appropriate terpene such as **7**.[23] Conversely, we envisioned a catalytic strategy that readily de-homologizes cyclic enolethers, such as **18**, (Fig. 4a + b) inspired by the work of Moulines et al.[41] Herein the authors describe the access to (–)-ambroxide **22** via a ketone intermediate resulting from sclareoloxide **14** in the presence of equivalent amounts of periodic and peracetic acids. We divided this transformation into two partial reactions, an iodine-mediated rearrangement and a peroxidative rearrangement (Fig. S16). First, both reactions were evaluated separately using enolether **18**. Evaluation of the iodide reaction conditions disclosed that catalytic (5 mol-%) amounts of sodium iodide in the presence of excess H_2O_2 (successively

added) and acidic buffer are enough to yield semi-pinacol rearrangement product **P-1** (60:40 *dr*) (Fig. 4c) almost quantitatively (97%). For the peroxidative rearrangement reaction, we employed the *candida antarctica* lipase (CALB) which is able to generate peracetic acid from H_2O_2 and ethyl acetate (EtOAc),[45] which served as the solvent simultaneously. As stated by the authors of ref. 41, the reaction had to be carried out at 50 °C and yielded lactone **1** with 70% in the best scenario (Fig. S16A). Conveniently, the oxidative rearrangement consumes both semi-pinacol diastereoisomers (Fig. S17). Finally, we combined both reactions in one pot using sclareoloxide **14** as the substrate EtOAc as the solvent and substituting sodium iodide with lugol's iodine (KI/I_2) to overcome solubility issues of the iodide catalyst. Careful evaluation of the reaction conditions led to the optimal setup consisting of 50 mM substrate shaken in EtOAc, 1 mol-% Lugol's iodine, 20 wt-% CALB, and 4 v/v-% 30% H_2O_2 (10 eq., successively added) at 50 °C for 5 h. Our proposed mechanism is depicted in Fig. 4c: Initially (i), CALB generates acetic and peracetic acid (AcOH and AcOOH) from water and EtOAc, which in combination with H_2O_2 is used for the acidic-oxidative generation of "I^+" (ii) (not further specified as iodine species are in a complex equilibrium).[46] The subsequently formed iodonium intermediate is then nucleophilically attacked by water to form a semiacetal, which immediately generates ketone intermediate **P-1** after deprotonation and semi-pinacol rearrangement (iii). **P-1** then forms a Bayer-Villiger product in the presence of AcOOH, generated by CALB, EtOAc, and H_2O_2 (i). After protonation, rearrangement, and cleavage of AcOH, the transient oxonium-ion reacts with $AcOO^-$, which in turn rearranges to form lactone **1** (iv).

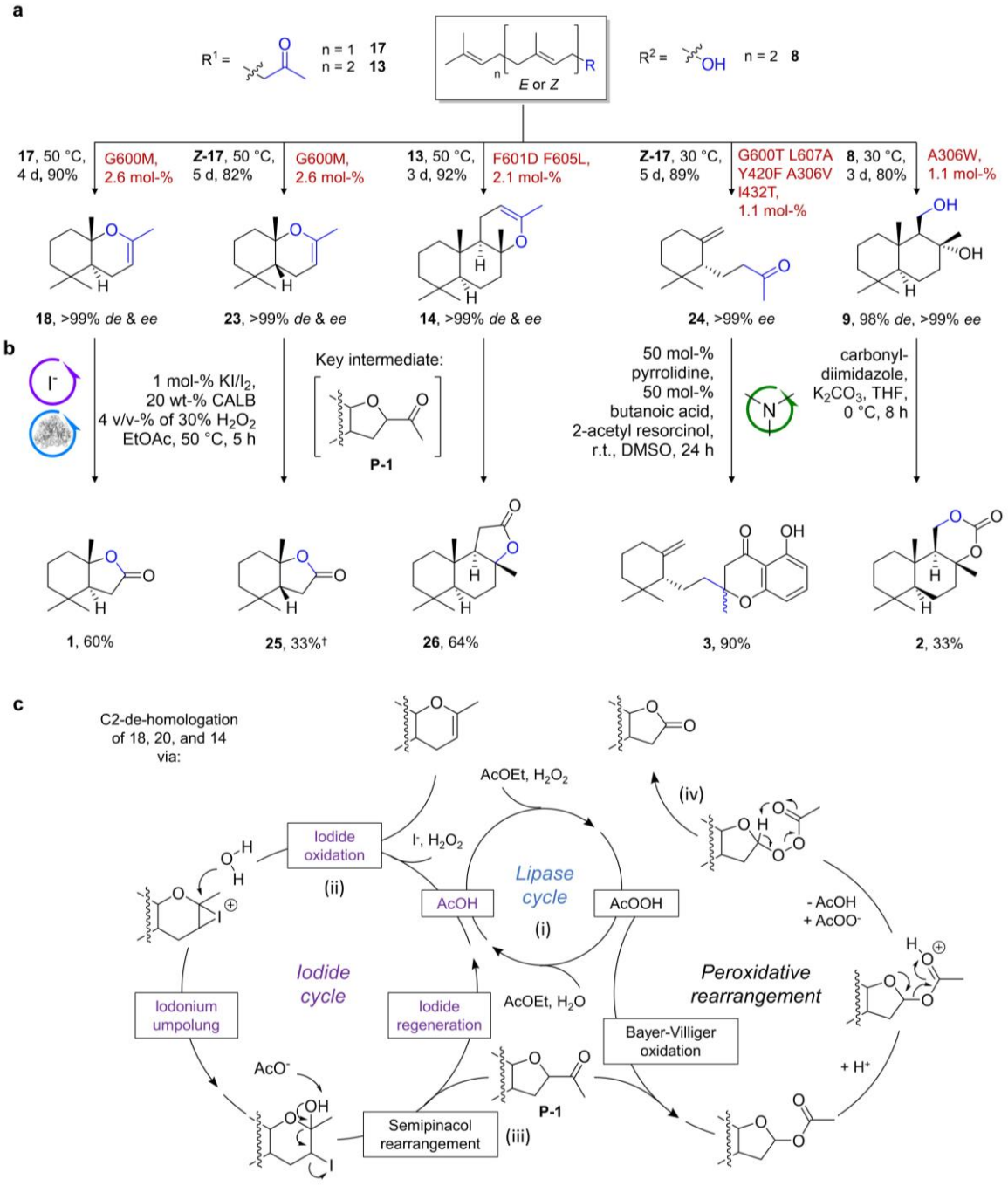

Figure 4: Modular hybrid syntheses of terpenes employing SHC biocatalysis (part 1). (A) Module 1, scaffold diversification: Biocatalytic generation of chiral cyclic terpenes 18, 23, 14, 24 and 9. (B) Module 2, scaffold derivatization: Interdisciplinary synthesis and catalysis to derivatize the chiral templates. (C) One-pot chemoenzymatic C2-dehomologation strategy of cyclic enolethers 18, 23 and 14 employing iodine and lipase catalysis (cf. Fig. S16 +17). For upscaling conditions and synthesis details please see supporting information. †determined via mesitylene standard.

Employing SHC biocatalysis, we cyclized **17**, ***Z*-17** and **13** to chiral enolethers **18**, **23**, **14** with high yields (82-92%) and subsequently edited their skeletal constitution using our iodine/lipase protocol to form *trans*-tetrahydroactinidiolide **1**, *cis*-tetrahydroactinidiolide **25** and (+)-sclareolide **26** with moderate yields of 33-64%. Next, (−)-γ-dihydroionone **24**, which was

prepared via directed cationic cyclization of ***Z*-17** with 89% yield, was coupled with 2-acetyl resorcinol in a pyrrolidine-catalyzed tandem aldol/ intramolecular Michael addition, also known as the Kabbe reaction, to generate chromanone **3** with 90% yield and 50:50 *dr*. Notably, L-proline and 2-methoxy-pyrrolidine were tested as alternative catalysts with potential stereocontrol over the Michael addition which, however, did not result in any conversion (data not shown). Solid drimen diol **9** was biocatalytically formed with a yield of 88% and transformed into carbonate **2** via potassium carbonate (K_2CO_3) mediated carbonylation with a moderate yield of 33%. Labdane **12** and *ent*-isocopolane **11** were also generated with high yields of 78% and 90%, respectively, from linear **10** and could potentially be transformed within three steps to sponge-derived meroterpenes **4** and **27** e.g., by transition metal-catalyzed cross-electrophile coupling of iodinated **12** and **11** with iodinated methoxy-benzoic esters as demonstrated in ref. 6. Finally, α-pyrone meroterpenes **28** and **29** that constitute the carbon skeleton of pyripyropenes and phenylpyropenes, were generated from chiral **16** and nicotinoic as well as benzoic ester in a base-mediated tandem γ-acylation/ intramolecular annulation reaction with yields of 64 and 28%, respectively (for a summary of the upscales see Table S3).

Conclusively, we could prove that the exquisite catalysis of cyclases can be harnessed for target-oriented synthesis of terpenes. Scaffold remodeling approaches to cyclic terpenes, while being testimonials of chemical creativity, can be shortened by up to 90% to essentially one diastereo- and enantiopure cyclization (cf. Fig. 2b), which is easily applicable as well as scalable, and provides yields up 92% at the same time. Combined with strategic interdisciplinary synthesis and catalysis we thus provided access to diverse terpenes in only two or three steps. Noteworthy, all devised routes comprised only commercially available substrates, and chirality was ensured by the shape-complementary substrate pre-folding in the SHCs active site. Thus, the stage is set for novel or drastically shortened retrosynthetic logic in de novo terpene synthesis.

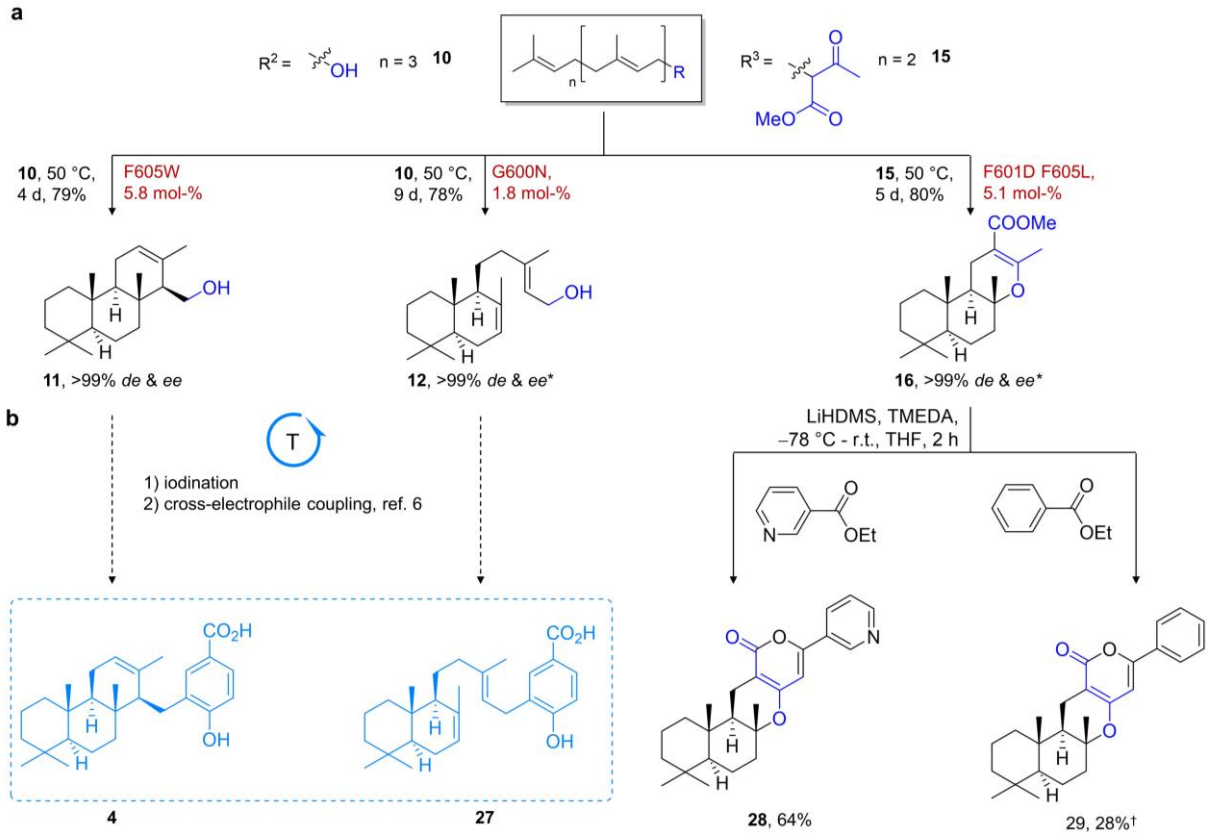

Figure 5: Modular hybrid syntheses of terpenes employing SHC biocatalysis (part 2). (A) Module 1, scaffold diversification: Biocatalytic generation of chiral cyclic terpenes 11, 12 and 16. (B) Module 2, scaffold derivatization: Potential strategy for meroterpenes 27 and 4, as well as the herein applied tandem γ-acylation/ intramolecular annulation to access α-pyrone meroterpenes 28 and 29. * assumed due to shape-complementary substrate prefolding in the SHC active site (Fig. S2) and circular dichroism data. Please see supporting information for reaction details. †determined via mesitylene standard.

Discussion

The golden age of biocatalysis enabled chemists to harness the catalytic power of enzymes, tailor them, and unlock their synthetic capabilities to streamline access to complex molecules. We herein provide the biocatalytic stereocontrolled head-to-tail cyclization as a tool in target-oriented terpene synthesis which has long been a methodological gap in synthetic logic and dates back to Ružička's demystification of terpene biogenesis.[47] The presented setup using bench-stable cell powder and encapsulating agents simplifies the application of these enzymes to the level of batch chemistry. The key herein is to mimic the new-to-nature conditions on a small scale, and adapt the system to inherent limitations, such as substrate hydrophobicity. Thus, this study also represents a helpful entry in the industrially oriented enzymology recently introduced by Woodley and coworkers.[42] Limitations of the presented strategy are still membrane diffusion issues which slow down the reaction and have been the target of earlier

studies.[48] Moreover, the enantioselectivity is determined due to the enzyme's active site which could be overcome by employing class II cyclases with inverted selectivity.[49] While debottlenecking the cationic head-to-tail cyclization, our hybrid routes disclosed challenges in fusing the cyclic templates to arene moieties. Therefore, it could be advisable to couple terpene and arene moiety prior to cyclization, as nature does, but at the expense of divergence potential.

Conclusion

The 'ideal synthesis' encompasses synthetic routes "[…] involving no intermediary refunctionalizations, and leading directly to the target […]".[50] *En route* to cyclic terpenes the stereocontrolled cationic cyclization genuinely epitomizes this overarching synthetic goal. Merging this tool with state-of-the-art synthesis and catalysis, such as electrochemical generation of the linear precursors[51] and biocatalytic remote oxidations[6] will further ease the access to complex terpenes. Moreover, harnessing the synthetic power of class I cyclases, will broadly expand the pool of accessible cyclic terpene scaffolds. Finally, we assume that hybrid strategies that leverage the best of both worlds - natural and man-made tools - will be a strong driving force in the pursuit of the ideal synthesis.

Acknowledgements

The authors thank Sven Richter for providing the reactor and Wendy Escobedo for introducing into Fluorescence microscopy. AS and BH gratefully acknowledge the Deutsche Forschungsgemeinschaft (DFG HA 1251/6-1) for research funding. NH thanks the Deutsche Forschungsgemeinschaft (DFG, German Research Foundation) for supporting this work by funding - EXC2075 – 390740016 under Germany's Excellence Strategy. NH and DM acknowledge the support by the Stuttgart Center for Simulation Science (SimTech), the High Performance and Cloud Computing Group at the Zentrum für Datenverarbeitung of the University of Tübingen, the state of Baden-Württemberg through bwHPC and the DFG through grant no INST 37/935-1 FUGG.

Author contributions

AS designed the project. AS and BH supervised the project. AS and TBL performed enzymatic reactions, fluorescence microscopy and upscaling studies. AS conducted substrate and product synthesis. DM and NH conducted free energy calculations.

Conflict of interest

The authors declare no conflict of interest.

References

1. Li, J., Amatuni, A. & Renata, H. Recent advances in the chemoenzymatic synthesis of bioactive natural products. *Curr. Opin. Chem. Biol.* **55**, 111–118 (2020).

2. Zetzsche, L. E., Chakrabarty, S. & Narayan, A. R. H. The Transformative Power of Biocatalysis in Convergent Synthesis. *J. Am. Chem. Soc.* **144**, 5214–5225 (2022).

3. Tetali, S. D. Terpenes and isoprenoids: a wealth of compounds for global use. *Planta* **249**, 1–8 (2019).

4. Corzo, D. *et al.* High-performing organic electronics using terpene green solvents from renewable feedstocks. *Nat. Energy* **8**, 62–73 (2022).

5. Maimone, T. J. & Baran, P. S. Modern synthetic efforts toward biologically active terpenes. *Nat. Chem. Biol.* **3**, 396–407 (2007).

6. Li, J., Li, F., King-Smith, E. & Renata, H. Merging chemoenzymatic and radical-based retrosynthetic logic for rapid and modular synthesis of oxidized meroterpenoids. *Nat. Chem.* **12**, 173–179 (2020).

7. Stout, C. N. & Renata, H. Reinvigorating the Chiral Pool: Chemoenzymatic Approaches to Complex Peptides and Terpenoids. *Acc. Chem. Res* **54**, 1143–1156 (2021).

8. Brill, Z. G., Condakes, M. L., Ting, C. P. & Maimone, T. J. Navigating the Chiral Pool in the Total Synthesis of Complex Terpene Natural Products. *Chem. Rev.* **117**, 11753–11795 (2017).

9. Lusi, R. F., Sennari, G. & Sarpong, R. Total synthesis of nine longiborneol sesquiterpenoids using a functionalized camphor strategy. *Nat. Chem.* **14**, 450–456 (2022).

10. Wishart, D. S. *et al.* DrugBank 5.0: a major update to the DrugBank database for 2018. *Nucleic Acids Res.* **46**, D1074–D1082 (2018).

11. Khan Kayani, W., Hafeez Kiani, B., Dilshad, E. & Mirza, B. Biotechnological approaches for artemisinin production in Artemisia. *World J. Microbiol. Biotechnol.* **34**, 54 (2018).

12. Romero-Suarez, D., Keasling, J. D. & Jensen, M. K. Supplying plant natural products

by yeast cell factories. *Curr. Opin. Green Sustain. Chem.* **33**, 100567 (2022).

13. Burlingame, A. L., Haug, P., Belsky, T. & Calvin, M. Occurrence of Biogenic Steranes and Pentacyclic Triterpanes in an Eocene Shale (52 Million Years) and in an Early Precambrian Shale (2.7 Billion Years): a Preliminary Report. *Proc. Natl. Acad. Sci. USA* **54**, 1406–1412 (1965).

14. Ishihara, K., Nakamura, S. & Yamamoto, H. The first enantioselective biomimetic cyclization of polyprenoids. *J. Am. Chem. Soc.* **121**, 4906–4907 (1999).

15. McCulley, C. H., Geier, M. J., Hudson, B. M., Gagné, M. R. & Tantillo, D. J. Biomimetic Platinum-Promoted Polyene Polycyclizations: Influence of Alkene Substitution and Pre-cyclization Conformations. *J. Am. Chem. Soc.* **139**, 11158–11164 (2017).

16. Arnold, A. M. *et al.* Enzyme-like polyene cyclizations catalyzed by dynamic, self-assembled, supramolecular fluoro alcohol-amine clusters. *Nat. Commun. 2023 141* **14**, 1–10 (2023).

17. Ungarean, C. N., Southgate, E. H. & Sarlah, D. Enantioselective polyene cyclizations. *Org. Biomol. Chem.* **14**, 5454–5467 (2016).

18. Christianson, D. W. Structural and Chemical Biology of Terpenoid Cyclases. *Chem. Rev.* **117**, 11570–11648 (2017).

19. Syren, P. O., Henche, S., Eichler, A., Nestl, B. M. & Hauer, B. Squalene-hopene cyclases - evolution, dynamics and catalytic scope. *Curr. Opin. Struct. Biol.* **41**, 73–82 (2016).

20. Eichhorn, E. *et al.* Biocatalytic Process for (-)-Ambrox Production Using Squalene Hopene Cyclase. *Adv. Synth. Catal.* **350**, 2339–2351 (2018).

21. Stephanopoulos, G., King, J. R., Edgar, S. & Qiao, K. Accessing Nature's diversity through metabolic engineering and synthetic biology. *F1000Research* **5**, 1–11 (2016).

22. Zeng, T. *et al.* TeroKit: A Database-Driven Web Server for Terpenome Research. *J. Chem. Inf. Model.* **60**, 2082–2090 (2020).

23. Serra, S. & Piccioni, O. A new chemo-enzymatic approach to the stereoselective synthesis of the flavors tetrahydroactinidiolide and dihydroactinidiolide. *Tetrahedron Asymmetry* **26**, 584–592 (2015).

24. Zhu, Y., Romain, C. & Williams, C. K. Sustainable polymers from renewable resources. *Nat. 2016 5407633* **540**, 354–362 (2016).

25. Yamashita, A. *et al.* Inhibitory effects of metachromin A on hepatitis B virus production

via impairment of the viral promoter activity. *Antiviral Res.* **145**, 136–145 (2017).

26. Brüggemann, M., Holst, C. & Hoppe, D. First enantioselective total synthesis of both (+)- and (-)-metachromin A. *European J. Org. Chem.* **4**, 647–654 (2001).

27. Lovering, F., Bikker, J. & Humblet, C. Escape from flatland: Increasing saturation as an approach to improving clinical success. *J. Med. Chem.* **52**, 6752–6756 (2009).

28. Basabe, P. *et al.* Synthesis of (+)-makassaric acid, a protein kinase MK2 inhibitor. *Tetrahedron* **66**, 6008–6012 (2010).

29. Sunazuka, T. & Omura, S. Total synthesis of α-pyrone meroterpenoids, novel bioactive microbial metabolites. *Chem. Rev.* **105**, 4559–4580 (2005).

30. Chen, K. & Baran, P. S. Total synthesis of eudesmane terpenes by site-selective C-H oxidations. *Nature* **459**, 824–828 (2009).

31. Schneider, A., Jegl, P. & Hauer, B. Stereoselective Directed Cationic Cascades Enabled by Molecular Anchoring in Terpene Cyclases. *Angew. Chem. Int. Ed.* **60**, 13251–13256 (2021).

32. Rauh, M. J. & Krystal, G. Synthesis of Pelorol and Analogues: Activators of the Inositol 5-Phosphatase SHIP ORGANIC LETTERS. *Biochem. Soc. Trans* **31**, 3 (2003).

33. Kühnel, L. C., Nestl, B. M. & Hauer, B. Enzymatic Addition of Alcohols to Terpenes by Squalene Hopene Cyclase Variants. *ChemBioChem* **18**, 2222–2225 (2017).

34. Hoshino, T., Kumai, Y., Kudo, I., Nakano, S. I. & Ohashi, S. Enzymatic cyclization reactions of geraniol, farnesol and geranylgeraniol, and those of truncated squalene analogs having C20 and C25 by recombinant squalene cyclase. *Org. Biomol. Chem.* **2**, 2650–2657 (2004).

35. Criswell, J., Potter, K., Shephard, F., Beale, M. H. & Peters, R. J. A single residue change leads to a hydroxylated product from the class II diterpene cyclization catalyzed by abietadiene synthase. *Org. Lett.* **14**, 5828–5831 (2012).

36. Morrone, D., Xu, M., Fulton, D. B., Determan, M. K. & Peters, R. J. Increasing complexity of a diterpene synthase reaction with a single residue switch. *J. Am. Chem. Soc.* **130**, 5400–5401 (2008).

37. Hua, S. K., Wang, J., Chen, X. B., Xu, Z. Y. & Zeng, B. B. Scalable synthesis of methyl ent-isocopalate and its derivatives. *Tetrahedron* **67**, 1142–1144 (2011).

38. Novaes, L. F. T., Gonçalves, K. D. A., Trivella, D. B. B. & Pastre, J. C. Formal Total Synthesis of Actinoranone: Synthesis Approaches and Cytotoxic Studies. *J. Org.*

Chem. **83**, 5160–5176 (2018).

39. Parker, K. A. & Resnick, L. The First Total Synthesis of a Pyripyropene-Type ACAT Inhibitor, (±)-GERI-BP00P. *J. Org. Chem* **60**, 5726–5728 (1995).

40. Seitz, M. *et al.* Synthesis of Heterocyclic Terpenoids by Promiscuous Squalene-Hopene Cyclases. *ChemBioChem* **14**, 436–439 (2013).

41. Moulines, J., Bats, J. P., Lamidey, A. M. & Da Silva, N. About a practical synthesis of Ambrox® from sclareol: A new preparation of a ketone key intermediate and a close look at its Baeyer-Villiger oxidation. *Helv. Chim. Acta* **87**, 2695–2705 (2004).

42. Erdem, E. & Woodley, J. M. Industrially useful enzymology: Translating biocatalysis from laboratory to process. *Chem Catal.* **2**, 2499–2505 (2022).

43. Allen, K. N., Entova, S., Ray, L. C. & Imperiali, B. Monotopic Membrane Proteins Join the Fold. *Trends Biochem. Sci.* **44**, 7–20 (2019).

44. Reetz, M. T., Soni, P., Fernández, L., Gumulya, Y. & Carballeira, J. D. Increasing the stability of an enzyme toward hostile organic solvents by directed evolution based on iterative saturation mutagenesis using the B-FIT method. *Chem. Commun.* **46**, 8657–8658 (2010).

45. Rüsch Gen. Klaas, M., Steffens, K. & Patett, N. Biocatalytic peroxy acid formation for disinfection. *J. Mol. Catal. B Enzym.* **19**–**20**, 499–505 (2002).

46. Bruchertseifer, H., Cripps, R., Guentay, S. & Jaeckel, B. Analysis of iodine species in aqueous solutions. *Anal. Bioanal. Chem.* **375**, 1107–1110 (2003).

47. Ruzicka, L. The isoprene rule and the biogenesis of terpenic compounds. *Exp. 1953 910* **9**, 357–367 (1953).

48. Benítez-Mateos, A. I., Schneider, A., Hegarty, E., Hauer, B. & Paradisi, F. Spheroplasts preparation boosts the catalytic potential of a squalene-hopene cyclase. *Nat. Commun.* **13**, 1–9 (2022).

49. Moosmann, P. *et al.* A monodomain class II terpene cyclase assembles complex isoprenoid scaffolds. *Nat. Chem.* **12**, 968–972 (2020).

50. a) Gaich, T. & Baran, P. S. Aiming for the ideal synthesis. *J. Org. Chem.* **75**, 4657–4673 (2010). b) J. B. Hendrickson, *J. Am. Chem. Soc.* **1975**, *92*, 5784–5800.

51. Harwood, S. J. *et al.* Modular terpene synthesis enabled by mild electrochemical couplings. *Science* **375**, 745–752 (2022).

TOC Figure

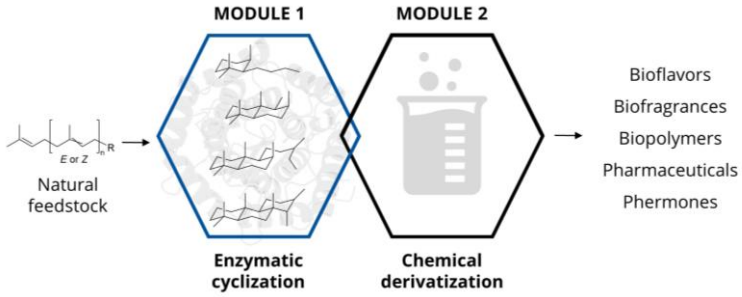
MODULE 1
MODULE 2
E or Z
n
R
Natural feedstock
Enzymatic cyclization
Chemical derivatization
Bioflavors
Biofragrances
Biopolymers
Pharmaceuticals
Phermones